Thermophysical properties of n-dodecane over a wide temperature and pressure range via molecular dynamics simulations with modification methods

Zhixia He[a], Yuanyuan Shen[a], Chuqiao Wang[b,*], Yanzhi Zhang[a], Manolis Gavaises[c]

[a] *Institute for Energy Research, Jiangsu University, Zhenjiang 212013, P.R. China*

[b] *School of Energy and Power Engineering, Jiangsu University, Zhenjiang 212013, P.R. China*

[c] *School of Mathematics, Computer Science and Engineering, City, University of London, UK*

Abstract The proposal of carbon peak and carbon neutrality has put forward new requirements for the expansion of the application conditions for hydrocarbon fuel thermophysical properties. The working range of hydrocarbon fuel has gradually expanded to high pressure/high temperature conditions even above the critical point. In this study, the density, internal energy, enthalpy, entropy, thermal conductivity and viscosity of n-dodecane molecular system are calculated using the SKS-UA force field in the isothermal-isobaric (NPT) ensemble via molecular dynamics (MD) simulations in the range of temperatures from 298 K to 2000 K and pressures from 1.2773 atm to 3000 atm. Three modification methods in terms of stability modification, kernel density estimation (KDE) modification and zero potential energy surface modification are proposed to improve the calculation accuracy of thermophysical properties. Average absolute relative deviation (AARD) and standard error (SE) are employed to perform error and uncertainty analysis on existing and non-existent thermophysical properties data of n-dodecane, respectively. The results indicate that the modified results for the six thermophysical properties are better than the uncorrected data. The modified density, internal energy, enthalpy, entropy, and thermal conductivity are in good agreement with the experimental values, while the viscosity is underestimated at low temperature. The thermophysical properties change drastically near the critical point. Among the environmental factors, pressure has a greater impact on density and thermal conductivity, while internal energy, enthalpy and entropy are more sensitive to temperature. Viscosity only changes significantly when the temperature below the critical point. This research method offers high-precision thermophysical property calculation results, inspiring the predictions of thermophysical property over a wide temperature and pressure range.

Key words n-dodecane; thermophysical properties; kernel density estimation modification; zero potential energy surface modification; wide range; molecular dynamics simulations;

1. Introduction

With the proposal of the "dual carbon" strategy, the realization of high-quality economic development and the goal of carbon peaking and carbon neutrality have put forward new requirements for the application of hydrocarbon fuels under extreme working conditions, for instance, ultra-high pressure and temperature[1-3]. When the temperature and pressure of the liquid fuel exceed a certain value which is corresponding to critical point, the gas-liquid interface disappears and becomes a homogeneous system. Above the critical point, hydrocarbon fuels are extremely sensitive to temperature and pressure changes, featured by dual liquid-gas characteristics, and unique thermophysical properties[4-7]. In conventional power machinery, the working range of hydrocarbon fuels is always below the critical point. However, with the energy

saving and emission reduction targets required by "dual carbon", the working range of hydrocarbon fuels has gradually expanded to ultra-high temperature and pressure circumstances above the critical point. As a result, extensive research into the thermophysical properties of hydrocarbon fuels over a wide temperature and pressure range is required.

Usually, there are two major methods to calculate the thermophysical properties of hydrocarbon fuels. One is from the macroscopic aspect, mainly based on the (semi) empirical model of the equation of state (EoS)[8]. The model parameters need to be adjusted according to various working conditions, and the parameters are primarily based on experience, resulting in limited calculation accuracy. While the second is from the microscopic aspect, especially the molecular dynamics (MD) approach[9]. Traditional molecular dynamics can examine intramolecular and intermolecular interactions from a microscopic perspective to determine the fuel molecular system's thermophysical characteristics. Molecular dynamics, compared to the equation of state, can essentially reflect the microscopic mechanism of thermophysical properties without constantly modifying model parameters, which has greater practical significance.

Distinct literatures place different emphasis on the thermophysical properties of hydrocarbon fuels. In terms of density calculation, Ivan Koljanin et al.[10] adopted OPLS and TraPPE force fields to study the densities of pentane and hexane by the isothermal-isobaric (NPT) ensemble in the MD simulations. They found that the linear alkane densities for OPLS and TraPPE are within 3 % and 2 % of the experimental value, respectively. Papavasileiou et al.[11] evaluated the liquid density with 280 n-dodecane molecules using atomistic and Coarse-Grained force fields over a broad temperature range from 323.15 K to 573.15 K at ambient pressure and obtained results were in good agreement with experiments data. Among all the simulated conditions, the density prediction using the united-atom (UA) force fields was generally more accurate and typically less than 5 % when compared to the experimental values reported by James et al[12]. Nikolay et al.[13] used the COMPASS to simulate the density of 2,2,4-trimethylpentane and found that this force field overestimated its density by 1.5-2 % near 500 MPa.

In terms of energy properties, there are comparatively few studies using MD simulations to calculate them[14-19]. Internal energy[14] is frequently utilized in MD simulations as a criterion for determining whether the system is stable or not, and it is also employed as a transition parameter for computing other physical parameters. While the enthalpy is generally expressed in the form of the enthalpy of evaporation. Zahariev et al.[15] demonstrated that the Amber force field accurately shows good reproduction of heat of vaporization of n-pentane, n-hexane, and n-heptane at different temperatures. Tomás Rego et al.[16] found the two state points of propyne employed in the optimization of the OPLS-AA force field have the highest variances, up to 10 % in vaporization enthalpy. In the study of Dmitrii et al.[17], 314 vaporization enthalpies of 155 hydrocarbons were determined between 240 K and 650 K and the simulated results agreed with the experimental data for the majority of the compounds. The thermodynamic integration approach was used to determine entropy through MD simulation, according to Kim Sharp et al.[18], and the change in total entropy of the molecular system were calculated more correctly. From a statistical mechanics perspective, Dimas Suárez et al.[19] employed the direct entropy method to assess the configurational entropy of individual molecules, enabling molecular simulations to present more complete pictures and new correlations.

In the study of MD thermophysical properties, most researchers focus on the calculation of transport properties, and a large number of literatures[20-24] on MD calculation of transport

properties have emerged. Maurizio and Gary et al.[20] calculated the viscosity of n-decane and n-hexadecane using the Green-Kubo together with Einstein methods confirming the equivalence of the two. Guilherme et al.[21] proved that most force fields do not accurately reproduce the viscosity of n-dodecane, except for the GROMOS force field, which is relatively superior. Yang et al.[22] predicted the viscosity of n-decane, n-undecane and n-dodecane in the canonical ensemble under sub/supercritical conditions and the predicted results were significantly underestimated. Unlike the previous three, Galliero et al.[23] and Chen et al.[24] conducted MD simulations to compute the transport parameters of n-alkanes, including thermal conductivity and viscosity. They discovered that viscosity was well estimated expect at low temperatures whereas thermal conductivity was consistently underestimated and transport properties correspond well with experimental data in conditions distant from the critical point, but not in neighborhood of it.

Many MD studies have been reported to focus on the thermophysical properties of hydrocarbon fuels in various power engineering fields[10-24], but there are still some deficiencies. First, classical MD simulations in the thermophysical properties of hydrocarbon fuels are not able to provide high enough computational precision. Except for density, the MD calculation results of other thermophysical properties deviate significantly from the experimental values. Secondly, in internal combustion engines, it has become an established trend to utilise high pressure common rail fuel systems in order to meet the dual-carbon challenge; the current experimental techniques are limited. Currently, it is nearly impossible to extend the operating conditions to high temperature and high pressure over the critical point to investigate the fuel thermophysical properties in practical experiments.

Motivated by all the above challenges, we explored the thermophysical properties of n-dodecane, a commonly single-component surrogate fuel for diesel in internal combustion engines, under a wide range of temperature and pressure conditions. Thermodynamic and transport properties are subsets of thermophysical properties. It is well known that the National Institute of Standards and Technology (NIST)[25] database is currently recognized as a relatively comprehensive database of fuel thermophysical properties. Therefore, for error analysis, NIST database will be used as the baseline to verify the results of various properties obtained in this study. To overcome the first deficiency, Seyed Aliakbar et al.[26] proposed a density plot of transport properties with temperature to improve the calculation accuracy. Based on this, the author proposes a kernel density estimation (KDE)[27-28] modification method for the working condition relationship to obtain accurate temperature and pressure. The KDE approach can investigate the data distribution characteristics of a data sample in order to precisely pinpoint the working condition range, thereby reducing the working condition fluctuation and the resultant thermophysical properties calculation errors. For energy properties, the energy property value at the standard boiling point of saturated liquid in the NIST database is 0, which is different from that in molecular dynamics software. Therefore, it is necessary to correct the zero potential energy surface[29] to achieve the purpose of the calculated value being consistent with the experimental value. The calculation is extended to a wide range of temperatures and pressures after the verification of existing data, and the corresponding thermophysical properties are obtained, thereby solving the second issue.

The paper is organized as follows: in Section 2, the method and details of MD simulation are introduced. On this basis, three modification methods, namely stability correction, KDE correction and zero potential energy surface correction, are combined to correct the acquired preliminary

thermophysical property results. Section 3 presents the calculation results for the thermophysical properties of n-dodecane derived using the method in this study and some special operating points regarding phase transitions and error manifestations are analyzed in the calculation process. Furthermore, error analysis and prediction under high temperature and high pressure are carried out for each thermophysical property. Finally, some conclusions are stated in Section 4 and supplementary data are offered at the end of the article.

Nomenclature	
Abbreviations	
MD	molecular dynamics
NPT	isothermal-isobaric
KDE	kernel density estimation
AARD	average absolute relative deviation
SE	standard error
EoS	equation of state
UA	united-atom
AA	all-atom
NIST	National Institute of Standards and Technology
GK	Green-Kubo method
MP	Muller-Plathe method
EMD	equilibrium molecular dynamics
RNEMD	reverse non-equilibrium molecular dynamics
LAMMPS	Large-scale Atomic/Molecular Massively Parallel Simulator
HACF	heat flux auto-correlation function
SACF	stress auto-correlation function
Symbols	
U	energy of the molecular system
E_{total}	internal energy
H	enthalpy
S	entropy
N	number of molecules
V	system volume
P	system pressure
T	system temperature
$\mathbf{J}$	heat flux
Greek letters	
ε	the potential well depth
σ	size parameters
φ	dihedral torsion angle

θ	bond angle
ρ	density
α	friction coefficient
κ	thermal conductivity
η	shear viscosity
τ	pressure tensor
Subscripts	
i, j	site number
x, y, z	Cartesian coordinates
α, β	position in the pressure tensor

2. Methodology

In this section, the force field for calculating and analyzing molecular system interactions of n-dodecane via MD simulations will be introduced first. After that, the method for calculating the thermodynamic properties and transport properties of n-dodecane will be described in turn. Then, we will present the relevant details of the MD simulation including the ensemble, initial configuration, system size, boundary conditions, etc. Finally, three correction methods for modifying the initial results obtained by classical MD simulation will be proposed.

2.1 Force field

For liquid n-alkanes, a variety of force fields have been investigated in many studies. Rajdeep et al.[30] found that the experimental values could be well reproduced regardless of the all-atom(AA) model or the united-atom(UA) model used to calculate the thermophysical characteristics of n-alkanes. However, due to the faster calculation speed and lower computational cost, the UA force fields were employed in our study. Comparing the accuracy of four different UA force fields, including OPLS-UA[31], SKS-UA[32], TraPPE-UA[33] and NERD[34], we adopted SKS-UA force field to describe molecular system interactions of n-dodecane in MD simulations.

Since alkane molecules are either non-polar or very weakly polar, charge or dipole moment effects are not considered, resulting in no Coulomb potential in the SKS-UA force field. Hence, the force field adopted in this article are as described as follows:

$$U_{total} = U_{bond} + U_{angle} + U_{dihedral} + U_{LJ}(r_{ij}) \quad (1)$$

where U_{total} is the total energy of the molecular system; U_{bond} and U_{angle} represent the bond stretching potential and angle bending potential, both of which are simple harmonic vibrations; $U_{dihedral}$ is the dihedral torsion potential and the style it adopts is opls; U_{lj} is the Lennard-Jones 12-6 potential used to describe the Van der Waals interaction[35]. In the SKS-UA force field, CH2 and CH3 are considered as pseudo-atoms or sites substituted for real atoms to complete the following energy calculations. The specific form each energy takes is shown in the following formula:

$$U_{bond} = \frac{1}{2} k_b (r_i - r_i^{eq})^2 \quad (2)$$

$$U_{angle} = \frac{1}{2} k_\theta (\theta_i - \theta_i^{eq})^2 \tag{3}$$

$$U_{dihedral} = V_0 + \frac{1}{2} V_1 (1 + \cos\varphi) + \frac{1}{2} V_2 (1 - \cos 2\varphi) + \frac{1}{2} V_3 (1 + \cos 3\varphi) \tag{4}$$

$$U_{LJ}(r_{ij}) = \begin{cases} 4\varepsilon_{ij} \left[\left(\frac{\sigma_{ij}}{r_{ij}} \right)^{12} - \left(\frac{\sigma_{ij}}{r_{ij}} \right)^{6} \right], & r_{ij} < r_c \\ 0, & r_{ij} \geq r_c \end{cases} \tag{5}$$

$$\varepsilon_{ij} = \sqrt{\varepsilon_{ii}\varepsilon_{jj}} \quad , \quad \sigma_{ij} = \frac{1}{2}(\sigma_{ii} + \sigma_{jj}) \tag{6}$$

where k_b is the bend stretching coefficient; r_i and r_i^{eq} are the bond length between two sites and its equilibrium value, respectively; k_θ is the angle bending coefficient; θ_i and θ_i^{eq} are the bond angle composed of three adjacent sites in a molecule and its equilibrium value, respectively; V_0, V_1, V_2, V_3 denote the dihedral torsion coefficient; φ is the dihedral torsion angle among four neighboring sites in the same molecule; r_{ij} is the distance between two non-adjacent sites on the same molecule or two sites on different molecules; r_c is cut-off distance, beyond which the Van der Waals interactions are ignored; ε_{ij} and σ_{ij} are the potential well depth and size parameters, respectively; For the potential well depth and size parameters between different kinds of sites, they are determined by the Lorentz-Berthelot mixing rule shown in Eq.(6). The values of mentioned parameters are shown in Table 1.

Table 1

Parameters of SKS-UA force field used in this study

Parameters	Units	Values
$\varepsilon_{CH3-CH3}$	$kcal/mol$	0.2265
$\varepsilon_{CH2-CH2}$	$kcal/mol$	0.0934
$\sigma_{CH3-CH3}$	Å	3.93
$\sigma_{CH2-CH2}$	Å	3.93
k_b	$kcal/mol \cdot Å^2$	191.77
r_i^{eq}	Å	1.54
k_θ	$kcal/mol \cdot rad^2$	124.15
θ_i^{eq}	°	114
V_0	$kcal/mol$	0.000
V_1	$kcal/mol$	1.411
V_2	$kcal/mol$	-0.271
V_3	$kcal/mol$	3.144
r_c	Å	15.0

2.2 Thermodynamic properties

In this section, thermodynamic properties of n-dodecane in the MD simulations include density ρ , internal energy E_{total} , enthalpy H and entropy S.

Density is an inherent property of the substance itself, which is related to factors such as the type of substance, system temperature and pressure. In this simulation, it can be directly obtained through a specific command provided by the software. The density ρ can be calculated as:

$$\rho = \frac{m}{V} = \frac{NM}{N_A V} \tag{7}$$

where N represents the number of molecules; M is relative molecular mass; N_A is Avogadro constant with a value of $6.02 \times 10^{23} mol^{-1}$; V is the system volume.

At present, there are few studies focusing on the calculation of energy properties for liquids, and most of them are used to evaluate the stability and convergence of the system. The main reason is that the specific calculated values of energy properties are not accurate enough, especially above the critical point. In the microscopic scale study, the internal energy E_{total} is the sum of the kinetic energy k_e and potential energy P_e of each site when the molecular internal structure does not break or change. Law of thermodynamics[36] can still be applied to calculate the enthalpy H in the microscopic scale according to the following expressions:

$$E_{total} = P_e + k_e = U_{total} + \sum_{i=1}^{N} (\frac{1}{2} m_i v_i^2) \tag{8}$$

$$H = E_{total} + PV \tag{9}$$

where m_i and v_i are the mass and velocity of the site i; P and V are the pressure and volume of the whole system.

For the entropy S, the coefficient α and the enthalpy H are added in the calculation formula as the change in entropy of the system by Kioupis et al.[37]. Due to its simplicity and versatility, the equations to calculate entropy S are employed below:

$$H = PV - \alpha \sum_i m_i v_i^2 \tag{10}$$

$$-\alpha \sum_i m_i v_i^2 = TS \tag{11}$$

where the coefficient α is a friction coefficient; T is the temperature of the system.

2.3 Transport properties

There are generally two methods to calculate transport properties in the MD simulations, namely Green-Kubo (GK) method[38] based on the equilibrium molecular dynamics (EMD) simulation and Muller-Plathe (MP) method[39] through the reverse non-equilibrium molecular dynamics (RNEMD). Applying the RNEMD method to calculate the viscosity of the liquid model and comparing the calculation results with the EMD method, Mao et al.[40] showed that the viscosity obtained by the RNEMD method was less accurate. Moreover, Yang et al.[41] found that the EMD methods showed better accuracy than the RNEMD methods in calculating thermal conductivity of hydrocarbon fuel. Thus, the GK method in the EMD simulation will be applied in the transport properties of n-dodecane in this paper.

The thermal conductivity κ is related to the ensemble average of the auto-correlation of the heat flux $\mathbf{J}$ by the GK formulas. The heat flux $\mathbf{J}$ consists of per-site kinetic energy, potential energy and stress in case of two-body interactions.

$$\kappa = \frac{V}{k_B T^2} \int_0^\infty \langle J_x(0) J_x(t) \rangle dt = \frac{V}{3 k_B T^2} \int_0^\infty \langle \mathbf{J}(0) \cdot \mathbf{J}(t) \rangle dt \tag{12}$$

$$\mathbf{J} = \frac{1}{V}\left[\sum_i e_i v_i - \sum_i \mathbf{S}_i v_i\right] = \frac{1}{V}\left[\sum_i e_i v_i + \frac{1}{2}\sum_{i<j}(\mathbf{F}_{ij}\cdot(v_i + v_j))r_{ij}\right] \quad (13)$$

where k_B is the Boltzmann constant with a value of $1.380649 \times 10^{-23}\mathrm{J/K}$; t is time; e_i is the per-site energy including kinetic and potential; $\mathbf{S}_i$ is the per-site stress tensor and $\mathbf{F}_{ij}$ is the interaction force between the site i and the site j.

Similarly, the GK approach will be used in the shear viscosity η calculation with the time integral of the ensemble average of stress tensor auto-correlation function.

$$\eta = \frac{V}{k_B T}\int_0^\infty \langle \tau_{\alpha\beta}(0)\tau_{\alpha\beta}(t)\rangle dt \quad (14)$$

where $\tau_{\alpha\beta}$ denotes the off-diagonal component $(\alpha \neq \beta)$ of pressure tensor which is a 3×3 matrix; α and β are the different elements of the x-, y-, z-directions; $<>$ represents the ensemble average of the auto-correlation function.

2.4 Simulation details

Each simulation was carried out in the Large-scale Atomic/Molecular Massively Parallel Simulator (LAMMPS)[42] package. The initial configuration, built via the software package Packmol[43], was the same for all simulations under distinct working conditions and was energy minimized using the Polak-Ribiere version of the conjugate gradient algorithm. A total of 3000 n-dodecane molecules (36000 sites with 6000 CH3 sites and 30000 CH2 sites) were generated in a three-dimensional cubic model with the system size of $230\text{Å} \times 220\text{Å} \times 220\ \text{Å}$ corresponding to the x-, y-, z-directions, respectively. The single molecular structure and the system mentioned above of the n-dodecane are shown in Fig. 1.

(a)

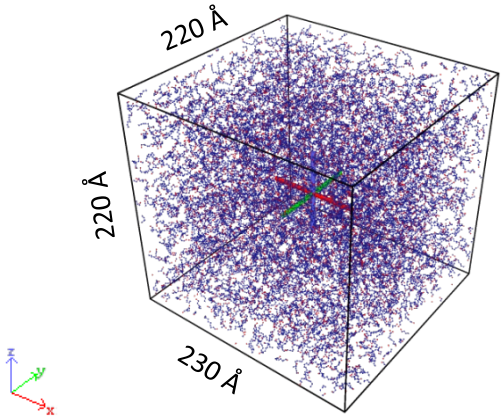

(b)

Fig. 1. The single molecular structure (a) and the cubic model system (b) of n-dodecane.

The velocity-Verlet algorithm was applied in the integration of Newton's equations of motion

with a timestep of 2 fs. Periodic boundary conditions were utilized in all directions, meaning that the sites can exit one end of the box and re-enter the other end when interacting across any boundary. The initial velocity of the system satisfied a Gaussian distribution at a given temperature to avoid too small or overlapping sites spacing. All simulations were performed in the NPT ensemble controlled by the time integration on Nose-Hoover style non-Hamiltonian equations of motion.

For thermodynamic properties, the relaxation was run initially for 1 ns with 500000 steps to obtain the system equilibrium in the NPT ensemble. Then, the system was switched to the calculation stage for 4 ns with sampling every 20 ps in the same ensemble. For transport properties, the simulation, sampling once under 20 fs interval and outputting an average value after 1000 times, was similarly relaxed for 1 ns and run for 4 ns with 2000000 steps. To avoid contingency in one run, all thermophysical properties were averaged over six independent runs by setting a random number of the seed to change the initial velocity.

2.5 Modification methods

2.5.1 Stability Modification

For the calculation of thermophysical properties of hydrocarbon fuels, stability modification has been adopted in a large amount of literature to optimize the calculation data to improve the calculation accuracy[44-46]. Different stability modification criteria are employed due to the distinction in the calculation methods of the thermodynamic properties and transport properties.

For the thermodynamic properties, it is necessary to evaluate whether the properties are in a convergent state or not by the fluctuation of the potential energy of the n-dodecane system in the simulations. In other words, the data after the moment when the potential energy of the system is almost unchanged are taken as the effective value for further calculations. Fig. 2 shows the relationship between the potential energy and the time of n-dodecane system at the pressure of 1.2773 atm and the temperature of 298 K. It is observed that the potential energy is converged after about 1 ns without great oscillation. Thus, the data after 1 ns are considered to be the corrected value of thermodynamic properties in the first step by stability modification.

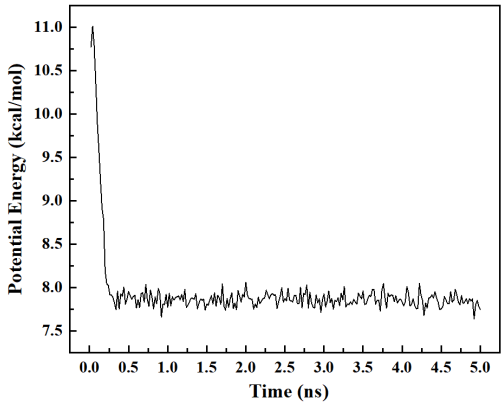

Fig. 2. Variation trend of potential energy with time in n-dodecane system at pressure of 1.2773 atm and temperature of 298 K.

Regarding the transport properties calculated by the GK method, the time needed for heat flux auto-correlation function (HACF) in the three directions decaying to zero is used to modify and calculate thermal conductivity at the given temperature and pressure. Meanwhile, the time for

stress auto-correlation function (SACF) in all directions converging to zero is employed in the modification of the viscosity under specified conditions. Fig. 3(a) shows the convergence of HACF with time in the n-dodecane system under high temperature and pressure. It can be seen from the figure that the HACF of the n-dodecane system converged very quickly and the HACF in each direction fluctuated around the line of HACF=0 within the range of ± 0.5 at the pressure of 1500 atm and temperature of 700 K. Hence, we took the data after the correlation time of 1.0 ns as the stability modification value of thermal conductivity. Fig. 3(b) shows the convergence of SACF with time in the n-dodecane system under the same conditions. When the SACFs in the xy-, yz-, zx-directions in the simulations are all converged or decay to zero, the time of 1.0 ns is enough for the viscosity calculation and modification. The convergence time are not the same under different working conditions whether in the HACF or SACF convergence. Therefore, the stability modification of transport properties needs to be carried out for each working condition, which is also used for thermodynamic properties. This is the first step of the correction, and the stability modification can ensure that the data is converged and the system is stable during the running stage.

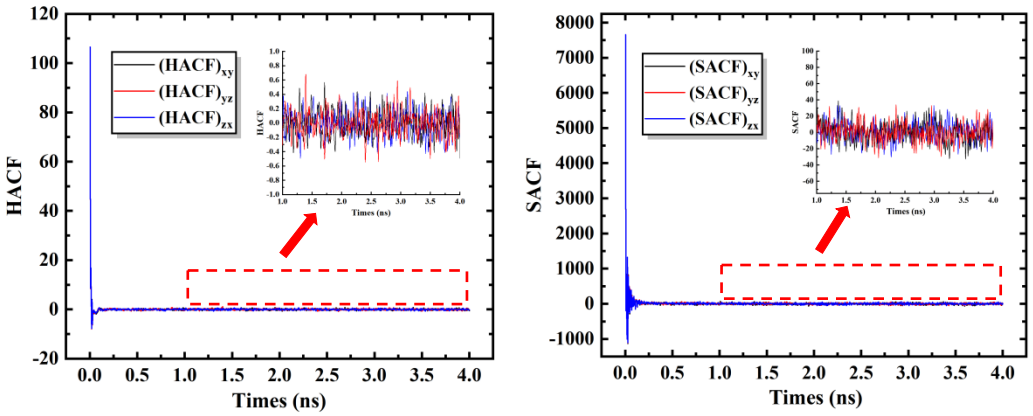

(a) (b)

Fig. 3. The convergence of HACF (a) and SACF (b) with time in the n-dodecane system at the pressure of 1500 atm and temperature of 700 K.

2.5.2 KDE Modification

At any input working condition, there are many data points of thermophysical properties of hydrocarbon fuels distributing around the preset conditions in the MD simulations. However, some data points deviate greatly from the preset operating conditions. If all data points are taken into account and averaged, the acquired thermophysical properties results are less accurate, especially under high temperature/high pressure conditions. This is a native defect in NPT ensembles causing large temperature and pressure fluctuations even if the system is set to a specific temperature and pressure in the MD simulations.

To solve this critical shortcoming, the KDE[27-28] modification method is proposed to improve the accuracy of the operating conditions obtained in the simulations. KDE method is able to study the data distribution characteristics from the data sample itself, so as to accurately locate the working condition range, narrow the working condition fluctuation range and reduce the thermophysical properties calculation errors caused by working condition fluctuation. In this study, we would combine the two-dimensional kernel density plot with the kernel density probability

distribution curve to make a two-dimensional marginal kernel density probability distribution plot. The plot at the pressure of 3000 atm and the temperature of 500 K is shown in Fig. 4. Every dot is a moment data including working condition and thermophysical properties. The color distribution represents the density of the pressure and temperature of all data points at every moment of one simulation and the kernel area marked in red is the place where the densest pressure and temperature distribution at the given working conditions. From the marginal kernel density probability distribution curve, it can also be seen where the most concentrated area of operating conditions is located. Therefore, the thermophysical properties data corresponding to the data points in the red kernel region or around the peak of the curve are selected as the effective data to further modify the thermophysical properties. In Fig. 4, it is observed that the useful data is in the kernel of the range of temperature at about 500 ± 2 K with pressure at 3000 ± 100 atm.

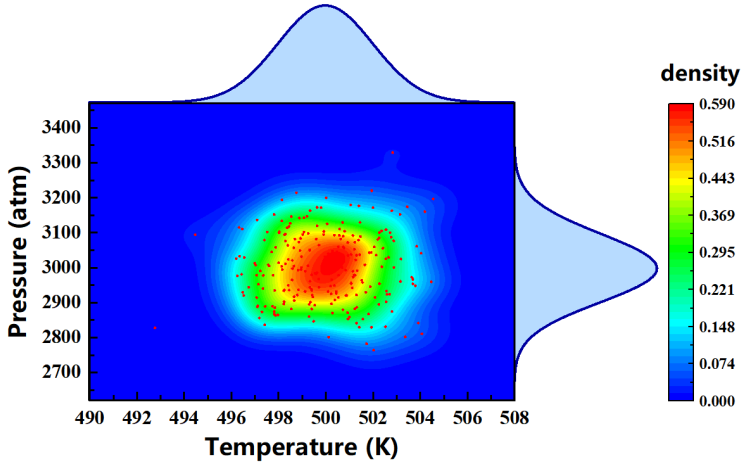

Fig. 4. The two-dimensional marginal kernel density probability distribution plot at the pressure of 3000 atm and the temperature of 500 K.

This is the second step of the modification, which is the correction of working conditions and applicable to the six thermophysical properties studied in our work. The final calculated values of density, thermal conductivity and viscosity over a wide temperature and pressure range can be determined by the stability modification and KDE modification mentioned above.

2.5.3 Zero potential energy surface modification for energy

In particular, an additional modification of the zero potential energy surface[29] is required for the calculation and correction of the energy properties including internal energy, enthalpy and entropy on the basis of the two steps mentioned above. The classical MD method often exhibits a trend consistent with the data obtained from experimental measurements when calculating energy properties, but there is a certain difference in the concrete numerical values even through the above stability modification and KDE modification. The reason for the difference is that the selections of the zero potential energy surface between simulations and experiments are distinct. In experiments, the energy properties values at the standard boiling point of saturated liquid are often defaulted to zero, while the LAMMPS software package has its own default zero potential energy surface. Simultaneously, the difference between the zero potential energy surfaces also varies with the system temperature. Thus, it is necessary to correct the zero potential energy surface of the energy properties in the MD simulations.

The specific implementation is as follows. According to the standard boiling point conditions of

n-dodecane in the saturated liquid phase, the MD simulations are carried out to acquire the calculated values of internal energy, enthalpy and entropy at the corresponding temperature and pressure. The calculated values of energy properties are equivalent to the differentials of the zero potential energy surface between the simulations and the experiments, since the experimental value of the energy properties under this condition is set as zero. Therefore, for the calculation of the internal energy, enthalpy, and entropy of n-dodecane under wide temperature and pressure conditions, the calculated values via MD method subtract the calculated value of the corresponding energy at the standard boiling point to obtain the final internal energy, enthalpy, and entropy data. This is the third step of the correction, specifically for the three energy properties of internal energy, enthalpy and entropy.

The final density, thermal conductivity and viscosity of n-dodecane can be obtained by combining the stability modification and KDE modification while the final internal energy, enthalpy and entropy of n-dodecane need to be acquired via integrating these two corrections and the zero potential energy surface modification.

3. Results and discussion

In this study, the thermophysical properties of n-dodecane at temperatures from 298 K to 2000 K and pressures from 1.2773 atm to 3000 atm in the MD simulations were calculated. 298 K and 1.2773 atm correspond to the working conditions under normal temperature and pressure, while 2000 K and 3000 atm are the maximum temperature that the fuel in the diesel engine nozzle can reach and the maximum injection pressure that the current diesel engine high-pressure common rail system can attain[47].

The temperature sampling points were set as 298 K, 500 K, 700 K, 1000 K, 1500 K and 2000 K respectively. The first three sampling points, the existing operating conditions in the NIST database, were mainly used to compare with the experimental values and verify the calculated values, and the latter three were extensions of higher temperature conditions. On the basis of the reliability of the verification results, the methods used in this study were applied to higher temperature conditions to predict the six thermophysical properties of n-dodecane at high temperature. The pressure sampling points were 1.2773 atm, 500 atm, 1000 atm, 1500 atm, 2000 atm, 2500 atm and 3000 atm, respectively. Similar to the temperature sampling points, only some operating points are provided with experimental data that can be used to verified, and others need to be predicted.

For the existing operating points in the NIST database, the corresponding experimental values are used to be compared with the calculated values via the MD simulations for error analysis of the results, mainly expressed by the average absolute relative deviation (AARD)[48]. The formula of AARD is as follows:

$$AARD = \frac{1}{n}\sum_{i=1}^{n}\frac{\phi_i^{MD} - \phi^{NIST}}{\phi^{NIST}} \times 100\% \tag{15}$$

where n is the number of independent runs of the MD simulations; ϕ_i^{MD} is the calculated value of a certain thermophysical property ϕ obtained by the ith independent run in MD simulations; ϕ^{NIST} is the corresponding experimental value in the NIST database.

The experimental data on the six thermophysical properties under the extreme working conditions are lacking when the sampling points beyond the range of working conditions in the NIST database. Therefore, the error analysis of the predicted thermal properties of n-dodecane

was carried out in the form of standard error (SE), which can properly quantify statistical errors and estimate the uncertainties of predicted values[49]. The expression of SE is written as:

$$SE = \frac{\sqrt{\sum_{i=1}^{n}(\phi_i^{MD} - \bar{\phi})^2}}{n} \tag{16}$$

where $\bar{\phi}$ is the average of the predicted values of a certain thermophysical property ϕ.

In this section, the error analysis of some special operating points will be introduced first, and then the calculation results of each thermophysical property of n-dodecane over a wide temperature and pressure range and the corresponding AARD and SE results will be given.

3.1 Thermophysical properties at special operating points

Some operating points possess experimental data that are convenient for verification while the others lack data among all the sampling points in this study. If the error values of these data points are represented on the same graph, there is no comparability and no practical significance.

The error expressions of the thermophysical properties of n-dodecane corresponding to different pressures are distinct at the sampling point of temperature of 298 K. At the temperature of 298 K, there is only properties at 1.2773 atm in the NIST database, and none at the other pressures. Thus, AARD is employed for error analysis at the pressure of 1.2773 atm, and SE is applied for other pressures. Therefore, their respective error manifestations and corresponding error values are clearly presented in the form of a table, as follows:

Table 2

The error manifestations and error values of each thermophysical property of n-dodecane under different pressures at the temperature of 298 K.

T (K)	P (atm)	Error Manifest-ations	Error values of properties (%)					
			ρ	E_{total}	H	S	κ	η
298	1.2773	AARD	-1.05	-0.33	-0.37	+30.67	-0.72	-59.06
	500	SE	0.005	0.13	2.42	0.43	0.60	0.001
	1000		0.003	0.29	3.71	0.97	0.39	0.004
	1500		0.007	0.49	1.65	1.66	0.79	0.007
	2000		0.007	0.35	4.52	1.17	0.66	0.009
	2500		0.005	0.49	1.92	1.64	0.80	0.01
	3000		0.16	0.61	2.45	2.05	0.36	0.007

In Table 2, the AARDs of the density, internal energy, enthalpy and thermal conductivity of n-dodecane at normal temperature and pressure are very small and mostly less than 1%. But the entropy and viscosity deviate more from the experimental values, the former overrated with a value of +30.67 % and the latter underestimated with a value of -59.06 %. Meanwhile, the SEs of properties are generally small, among which the density and viscosity are extremely small and

enthalpy is relatively large.

Similarly, the normal pressure of n-dodecane, i.e, 1.2773 atm, is also a special operating point in this study. First of all, only the thermophysical characteristics of n-dodecane at three temperatures of 298 K, 500 K, and 700 K are available in the NIST database under this pressure. Secondly, the phase state of n-dodecane in the MD simulations transforms with the change of temperature. Only at the temperature of 298 K and pressure of 1.2773 atm, n-dodecane system is liquid while other temperatures under this pressure are in gas phase. Therefore, the above two reasons lead to the differences in the error values of the calculated thermophysical properties under the pressure of 1.2773 atm. The detailed results are shown in Table 3.

Table 3

The phase states, error manifestations and error values of each thermophysical property of n-dodecane under different temperatures at the pressure of 1.2773 atm.

P (atm)	T (K)	Phase states	Error Manifestations	Error values of properties (%)					
				ρ	E_{total}	H	S	κ	η
1.2773	298	Liquid	AARD	-1.05	-0.33	-0.37	+30.67	-0.72	-59.06
	500	Gas	AARD	+5.08	-4.24	-2.58	-11.93	-77.97	-62.63
	700	Gas	AARD	+5.94	+0.02	+0.008	-22.92	-85.32	-72.41
	1000	Gas	SE	2.95E-04	0.94	2.84	0.94	0.05	1.66E-05
	1500	Gas	SE	4.55E-04	1.31	3.92	0.88	0.02	1.05E-05
	2000	Gas	SE	3.17E-04	2.82	4.29	1.41	0.05	1.38E-05

In Table 3, the n-dodecane is liquid at normal temperature and pressure and its density, internal energy, enthalpy and thermal conductivity are in good agreement with the experimental values. However, with the increase of temperature, the liquid n-dodecane gradually transforms into the gas phase. The deviations of the calculation results in the gas phase are larger than that in the liquid phase due to the large molecular distances and the instability of the gas phase system itself, such as thermal conductivity. However, it can still be seen that the consistencies of density, internal energy and enthalpy with the NIST data are very good. Since the calculation of entropy is based on the calculation result of internal energy, leading its error to be a cumulative error, the AARD of entropy is relatively large. The viscosity is far underestimated and its AARDs are up to 60 % whether in liquid phase or in gas phase. For the predicted thermophysical properties of n-dodecane, the SEs of enthalpy are still comparatively large.

3.2 Thermodynamic properties

The density results of n-dodecane over a wide temperature and pressure range obtained through the MD simulations by utilizing the two correction methods of stability modification and KDE modification are presented in Fig. 5(a). It can be seen that an obvious turning point is at around the temperature of 650 K, where a sudden change in density occurs. The critical temperature of n-dodecane is 658 K, which is exactly in line with such a point[50]. Thus, it can be induced that the

changes of density after the critical point with temperature and pressure are very huge due to the supercritical transformation. The variation trends of density with temperature and pressure are clearly revealed in Fig. 5(b). At the same temperature, the density of n-dodecane increases as the pressure rises. Only at 298 K is n-dodecane completely liquid. With the increase of temperature, n-dodecane under normal pressure turns into the gas phase, and at the other pressures, it is in a transition state between the two phases. In this state, the density drops uniformly with rising temperature at the same pressure.

For the density calculation for n-dodecane, since there are density data at 500 K and 700 K in the NIST database, AARDs are used for error analysis on the MD calculated values; while there is no experimental data from 700 K to 2000 K, SEs are applied for analysis.

Fig. 6 shows the comparison among the data from NIST database, uncorrected and modified MD calculations for the density of n-dodecane at temperatures of 500 K and 700 K under different pressures. The black lines represent the density data under the corresponding conditions in the NIST database[25], and the red dots represent the modified results using the method in this study while the blue dots are the uncorrected calculations directly by conventional MD simulations. There is essentially no difference between the uncorrected and corrected values for this thermophysical property. The pink numbers indicate AARD values between NIST database and modified calculations. At a temperature of 500 K, the AARD of density is a maximum of +0.93 % at a pressure of 3000 atm and a minimum of -0.09 % at 1000 atm. At a temperature of 700 K, AARD is the largest at a pressure of 500 atm with a value of -0.80 %, and at a pressure of 2000 atm is the smallest with a value of +0.0005 %. Among all of these operating points, the AARDs in the density calculation of n-dodecane are all less than 0.93 %, meaning the corrected density calculations that are in good agreement with NIST database can be obtained in this study.

Fig. 7 presents a 3D waterfall plot of the SE values for the density calculations for each sampling point of n-dodecane at different pressures and the temperatures ranging from 700 K to 2000 K. Different line colors represent different temperatures, and a series of dots represent the SEs of the modified MD calculated values at all sampling points. It can be seen from the figure that the SEs of density calculations are not provided with a definite trend with temperature and pressure conditions, but the values of SEs are very small, all below 0.03 %.

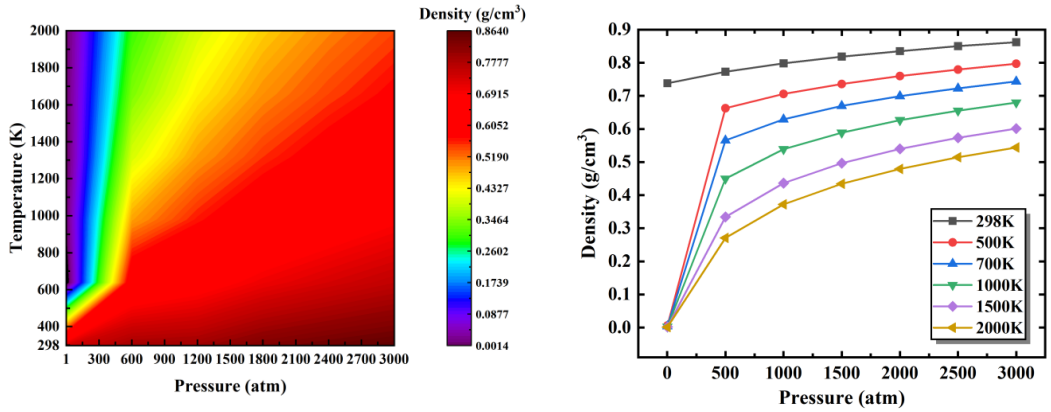

(a) (b)

Fig. 5. The modified results and variation trends of the density for n-dodecane in the range of temperature from 298 K to 2000 K and pressure from 1.2773 atm to 3000 atm.

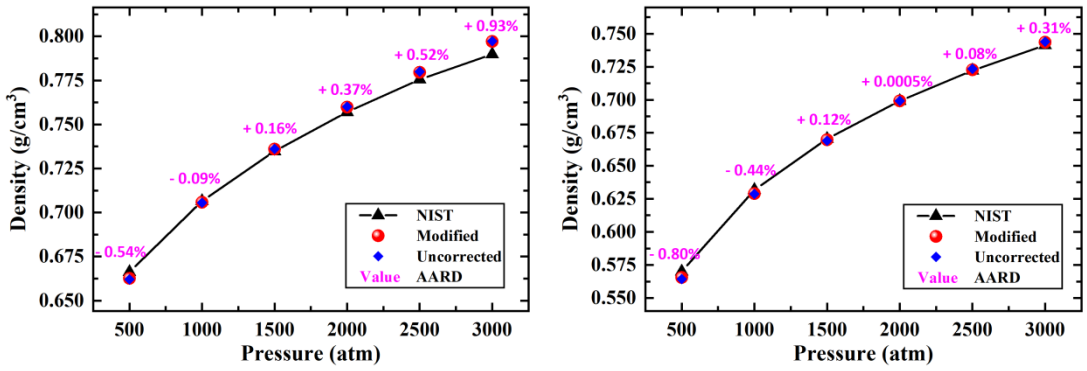

(a) T=500K (b) T=700K

Fig. 6. The comparison of NIST data, uncorrected and modified MD calculations for the density of n-dodecane at the temperatures of 500K and 700K under different pressures. The pink number indicates AARD value at each operating point between the NIST data and modified MD calculations.

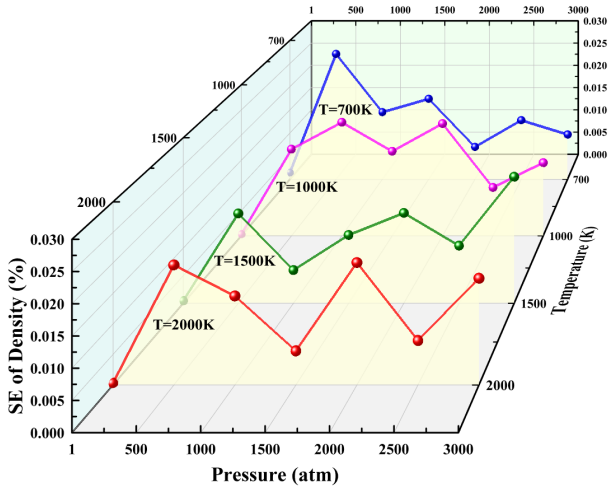

Fig. 7. The SEs of the density calculations for each sampling point of n-dodecane at different pressures and the temperatures ranging from 700 K to 2000 K. Different line colors represent different temperatures, and a series of dots represent the SEs of the modified MD calculated values at all sampling points.

For the acquisition of energy properties, the calculation results of the internal energy, enthalpy and entropy are obtained through the combined action of stability modification, KDE modification and zero potential energy surface modification based on the preliminary MD simulations.

The modified results of the internal energy for n-dodecane over a wide temperature and pressure range by the MD simulations are shown in Fig. 8. It is simple to find that after the working conditions exceed the critical point, the changes of internal energy with pressure at the same temperature are very small and almost negligible. The more influential factor on internal energy calculations is temperature rather than pressure, which is also easy to understand. The increase of temperature makes the n-dodecane molecules in the system move more violently, impacting the distances between molecules directly, and thus the kinetic energy and potential energy of the system increase. Therefore, the internal energy of n-dodecane increases substantially with the increase of temperature, especially at high temperature conditions.

The variation trend of the internal energy for n-dodecane with pressure at the temperatures of

500 K and 700 K can be observed in Fig. 9. The internal energy value of n-dodecane at 500 K is basically around 0 kcal/mol. At a pressure of 500 atm, the MD calculated value of the internal energy is -0.44895 kcal/mol, while the NIST data is -0.263 kcal/mol, and the AARD between the two is +70.43 %. At this temperature, the minimum internal energy error of n-dodecane is -12.23 % at a pressure of 3000 atm, as shown by the pink numbers in the figure. The blue dots represent the preliminary calculation results of internal energy using traditional MD simulations. Compared with the uncorrected results, the corrected MD calculations are significantly closer to the experimental values and the error between the two is smaller. The modified results of internal energy at a temperature of 700 K are consistent with the experimental data, with an error range of -0.73 % to +0.11 %.

Fig. 10 indicates the results of the internal energy error for n-dodecane, i.e, SEs, at operating points not included in the NIST database. As seen from the figure, regardless of any temperature condition, the SEs of the internal energy at the pressure of 3000 atm are always relatively the highest. The overall error is comparatively larger at high temperatures even if there are a few points with smaller errors. However, the internal energy calculation errors of n-dodecane are still low overall, with SEs ranging from 0.44 % to 2.98 %.

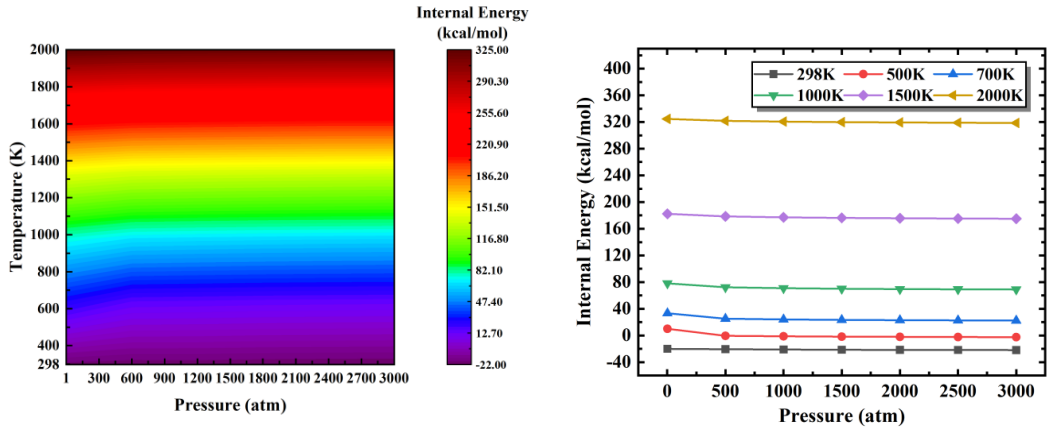

(a) (b)

Fig. 8. The modified results and variation trends of the internal energy for n-dodecane at the temperatures from 298 K to 2000 K and pressures from 1.2773 atm to 3000 atm using three modifications in the MD simulations.

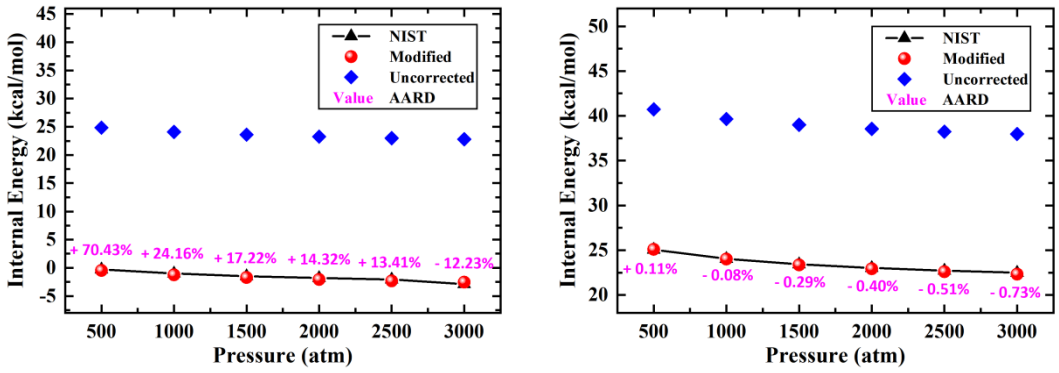

(a) T=500K (b) T=700K

Fig. 9. The comparison of NIST data, uncorrected and modified MD calculations for the internal

energy of n-dodecane at the temperatures of 500K and 700K under different pressures. The pink number indicates AARD value at each operating point between the NIST data and modified MD calculations.

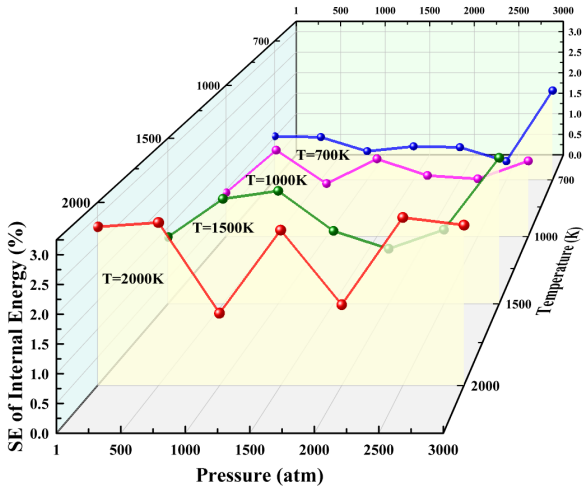

Fig. 10. The SEs of the internal energy calculations for each sampling point of n-dodecane at different pressures and the temperatures ranging from 700 K to 2000 K. Different line colors represent different temperatures, and a series of dots represent the SEs of the modified MD calculated values at all sampling points.

The modified results of the enthalpy for n-dodecane at the temperatures from 298 K to 2000 K and pressures from 1.2773 atm to 3000 atm using the same three modifications are illustrated in Fig. 11. The overall trend of the enthalpy calculation results is consistent with that of the internal energy. However, the trends of the two are slightly different after the critical point. Compared with internal energy, enthalpy has a small increase with pressure at the same temperature after exceeding the critical point condition. In other words, at the same temperature, there is an enthalpy minimum around the critical pressure. But as the temperature increases, the phenomenon is no longer that obvious. Therefore, temperature is still the more influential factor on enthalpy results than the pressure.

Fig. 12 demonstrates the calculated results and their AARDs of n-dodecane enthalpy at the temperatures of 500 K and 700 K. The change trends of enthalpy with pressure at the two temperatures are similar, and both increase with the rise of pressure, showing an approximate linear relationship. At a temperature of 500 K, the AARDs of enthalpy have a minimum value of -0.47 % at a pressure of 1500 atm, and a maximum value at a pressure of 3000 atm with a value of +3.07 %. When the temperature is 700 K, the AARDs of the enthalpy are generally lower than that at 500 K, and the minimum value is only +0.002 % while the maximum is just up to -0.48 %. It is not difficult to conclude that, similar to the internal energy, the corrected results of the enthalpy are more in line with the experimental values than the uncorrected ones.

Unlike other thermodynamic properties, the SE results of n-dodecane in enthalpy calculations have no regularity at all. The SEs of enthalpy present an unstable or even fluctuating state with variations in either temperature or pressure as shown in Fig. 13. However, the SEs of enthalpy are relatively larger, and their values fluctuate between 2.22 % and 10.15 %. In general, higher errors generally occur at higher temperature conditions.

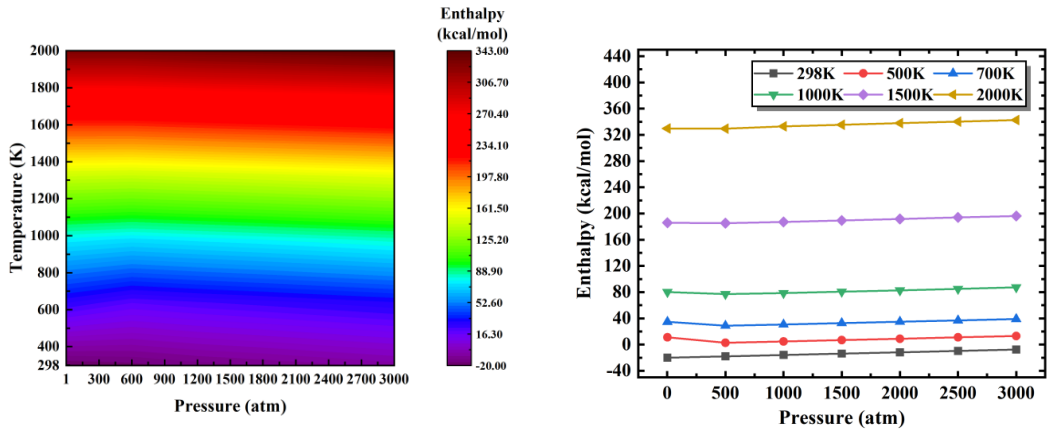

(a) (b)

Fig. 11. The modified results of the enthalpy for n-dodecane at the temperatures from 298 K to 2000 K and pressures from 1.2773 atm to 3000 atm using the same three modifications in the MD simulations.

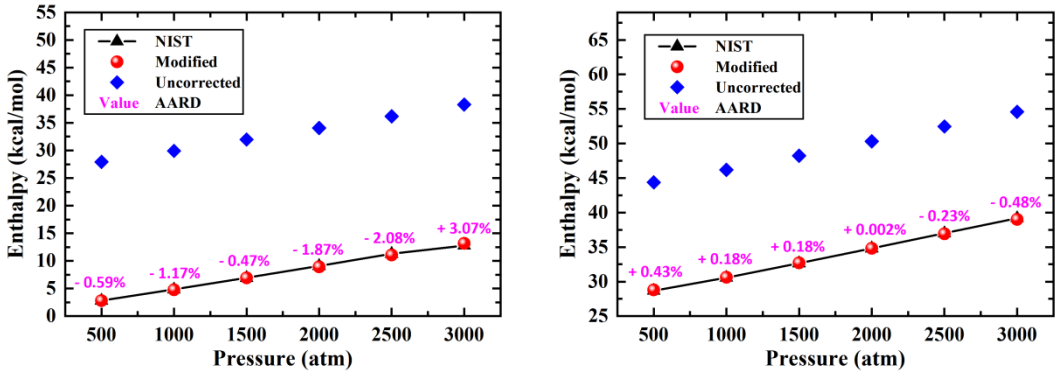

(a) T=500K (b) T=700K

Fig. 12. The comparison of NIST data, uncorrected and modified MD calculations for the enthalpy of n-dodecane at the temperatures of 500K and 700K under different pressures. The pink number indicates AARD value at each operating point between the NIST data and modified MD calculations.

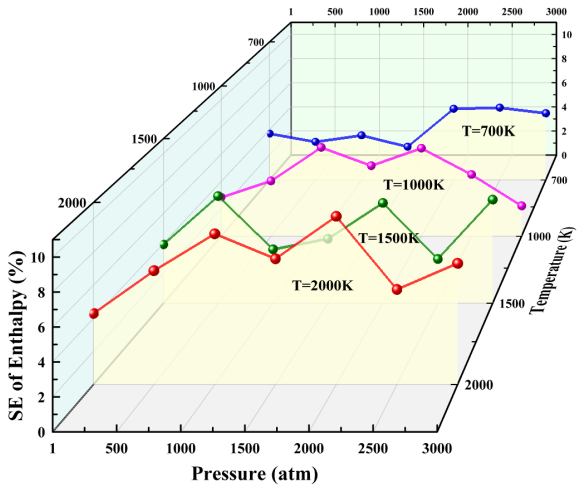

Fig. 13. The SEs of the enthalpy calculations for each sampling point of n-dodecane at different pressures and the temperatures ranging from 700 K to 2000 K. Different line colors represent

different temperatures, and a series of dots represent the SEs of the modified MD calculated values at all sampling points.

Fig. 14 shows the modified results of the entropy for n-dodecane by MD simulations combined with three correction methods over a wide temperature and pressure range. It can be found that with the increase of temperature, the entropy of n-dodecane increases rapidly at first and then turns to a uniform rise. Entropy drops steeply around the critical point, but when the pressure continues to increase, the entropy smooths out and begins to trend slightly downward. In general, entropy is less sensitive to system pressure and more influenced by temperature considerations, which is similar to the other two energy properties mentioned above.

The modified calculation results of the entropy for n-dodecane at 500 K and 700 K and their AARDs are shown in Fig. 15. Even if there are some differences with the experimental values regardless of the temperatures, it is preferable to employ the correction approach since the corrected entropy values are closer to the experimental value than the uncorrected ones. The AARDs of modified values in entropy calculations are relatively larger than other energy properties mentioned above, ranging from -29.54 % to +13.51 % at 500 K, and from -15.57 % to -10.38 % at 700 K. By dissecting the process of the entropy calculations via modification methods, it is not difficult to find that there are two possible reasons for this consequence. Firstly, the Eq.(10)-(11) used to calculate the entropy of n-dodecane depend on the calculation results of internal energy, thus causing the cumulative effect of calculation errors and making the entropy results less accurate. Secondly, the Eq.(10)-(11) are compared with the formulas adopted by others to calculate entropy using another software of MD simulations, GROMACS[51] package, and the difference between the two lies in the calculation of Helmholtz free energy[52-53]. Our work did not consider the influence of Helmholtz free energy, which may have a certain impact on the calculation results of entropy. These explanations are yet to be determined through further research and exploration.

It is necessary to observe the magnitudes of the entropy errors in the form of SEs at the temperature from 700 K to 2000 K and the pressure from 1.2773 atm to 3000 atm, as illustrated in Fig. 16. Comparing the SEs of the internal energy under the same working conditions (Fig. 10), it can be found that the variation trends of the two with pressure are basically the same, with a slightly distinct in specific values. It could be seen in Fig. 16 that the SEs at 2000 K are not significantly larger than those at other temperatures. All SEs of this thermodynamic property are below 3 %, and both the maximum and minimum values appear at the temperature of 700 K, where the maximum value is 2.98 % and the minimum value is 0.62 %.

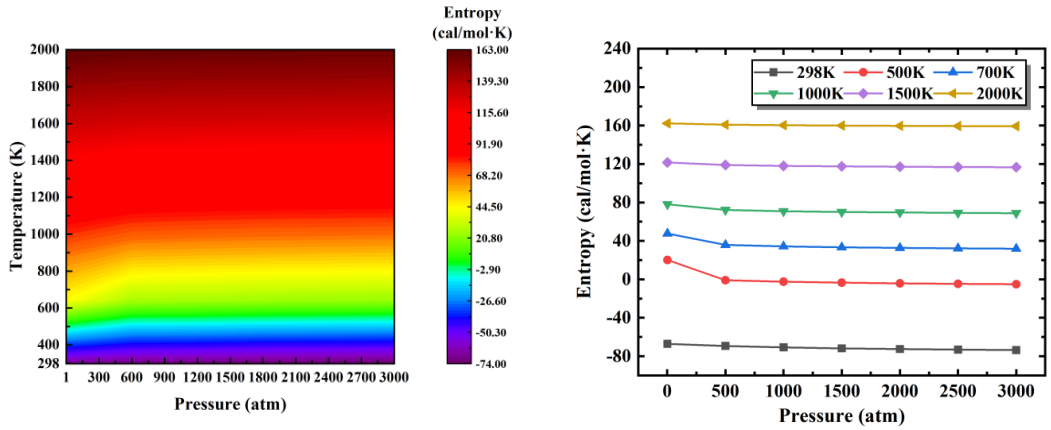

(a) (b)

Fig. 14. The modified results of the entropy for n-dodecane at the temperatures from 298 K to 2000 K and pressures from 1.2773 atm to 3000 atm using the same three modifications in the MD simulations.

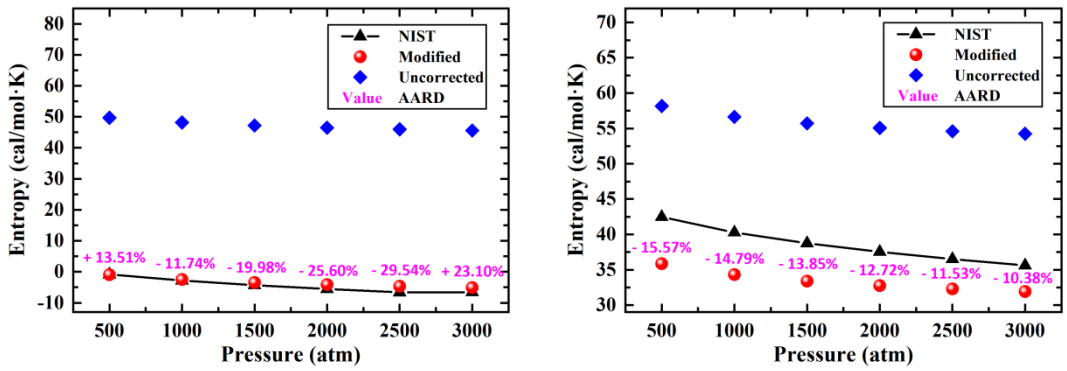

(a) T=500K (b) T=700K

Fig. 15. The comparison of NIST data, uncorrected and modified MD calculations for the entropy of n-dodecane at the temperatures of 500K and 700K under different pressures. The pink number indicates AARD value at each operating point between the NIST data and modified MD calculations.

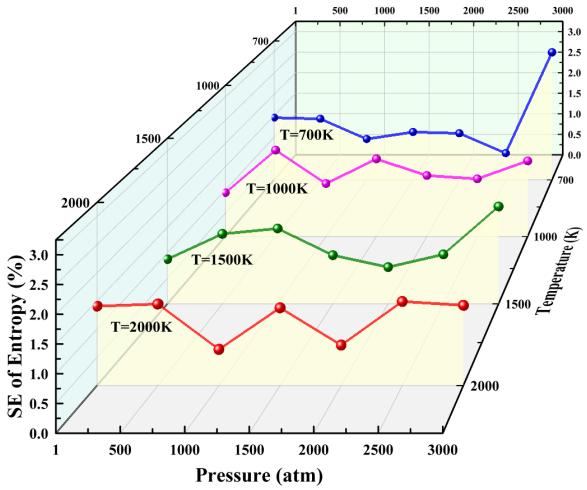

Fig. 16. The SEs of the entropy calculations for each sampling point of n-dodecane at different pressures and the temperatures ranging from 700 K to 2000 K. Different line colors represent different temperatures, and a series of dots represent the SEs of the modified MD calculated values at all sampling points.

Combining the calculation results of the above four thermodynamic properties over a wide temperature and pressure range, it can be found that all these thermodynamic properties of n-dodecane change dramatically after the critical point, whether it is suddenly decreased or abruptly increased. Therefore, a sharp turning point near the critical point[54] can be seen in the graph. All modified thermophysical properties are in better agreement with the experimental values than the uncorrected results, and AARD at low temperature is always larger than that at high temperature for errors in energy properties. The overall SE is the smallest in the density calculations, with a value below 0.03 %, and the largest in the enthalpy calculations, with a value of about 10 %. Detailed numerical data and errors of thermodynamic properties including density,

internal energy, enthalpy, and entropy over a wide temperature and pressure range are provided in Appendix A, where errors include AARDs and SEs.

3.3 Transport properties

The thermal conductivity of n-dodecane is simulated by the stability correction of the heat flux in all directions of the system and the KDE correction of the working conditions based on the MD methods. The results obtained are shown in Fig. 17. The minimum value of thermal conductivity appears in the gas phase region of normal pressure and high temperature, and the maximum value is in the region of high pressure and low temperature. Likewise, there is a sharp turning point near the critical point of n-dodecane. With the increase of the temperature, the thermal conductivity tends to decrease slightly; however, it is considerably affected by the pressure and the overall tendency is upward as the pressure rises. In the low pressure region, the thermal conductivity is more sensitive to pressure than that in the high pressure region. This is analogous to the trend of the density with working conditions.

For the existing operating conditions in the NIST database, the results obtained in this study are compared to the thermal conductivity data in the NIST database, and the consequences are shown in Fig. 18. Black line represents the results from the NIST database, red dots are the values obtained by both correction methods, and blue dots indicate the values acquired using preliminary MD simulations. For thermal conductivity, the corrected calculations are also markedly superior to the uncorrected results. The difference between the modified results and the experimental values is significantly reduced, where the AARD range from -3.60 % to +0.83 % at 700 K and from -1.68 % to -0.11 % at 500 K, as indicated by the pink numbers in the figure. At a temperature of 500 K, due to the lacking thermal conductivity data under high pressure in the NIST database, it is expressed in the same error form of SE as the predicted data. The corresponding SE under the pressure of 2500 atm is 0.47 %, and under the pressure of 3000 atm is 0.63 %.

The SE results of the thermal conductivity prediction data for n-dodecane are illustrated in Fig. 19. It can be seen that at the same temperature, with the increase of pressure, the error of thermal conductivity increases correspondingly, except for the temperature of 1500 K. At this temperature, SE results fluctuate with the increase of pressure, but also tend to increase in general. Even so, the SEs of the thermal conductivity under all conditions is minimal, not exceeding 0.7 %.

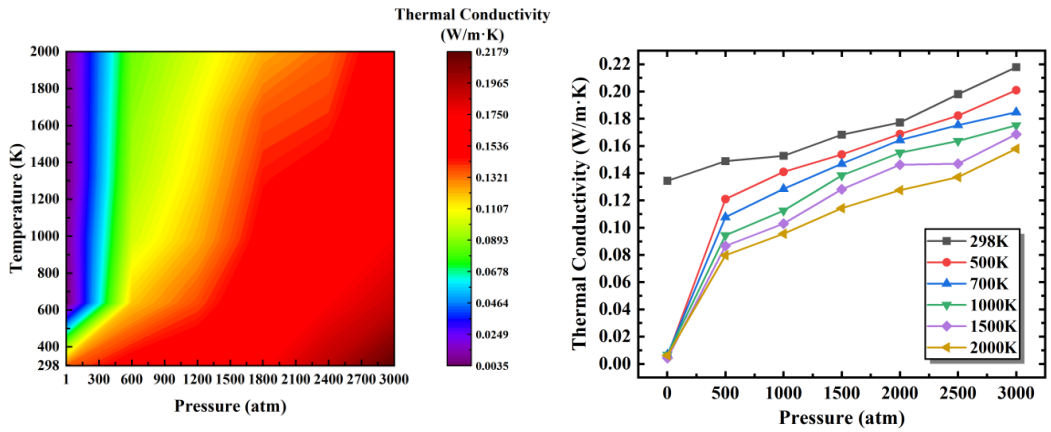

(a) (b)

Fig. 17. The modified results of the thermal conductivity for n-dodecane at the temperatures from 298 K to 2000 K and pressures from 1.2773 atm to 3000 atm using the stability and KDE

modifications in the MD simulations.

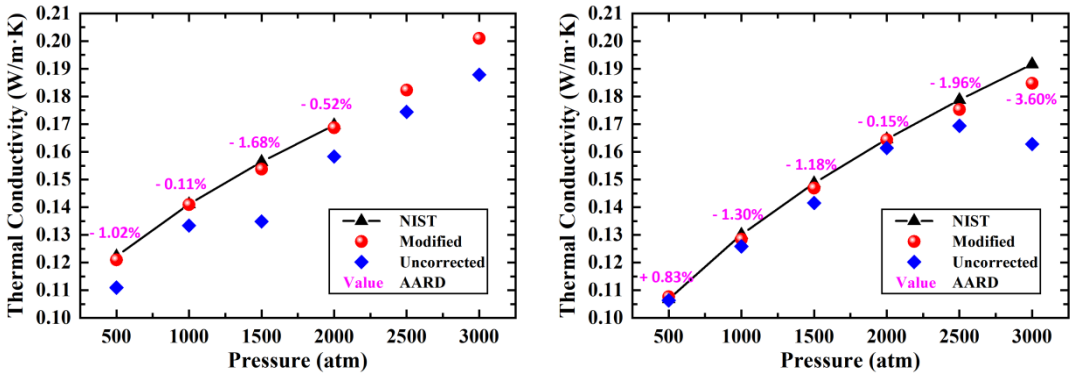

(a) T=500K (b) T=700K

Fig. 18. The comparison of NIST data, uncorrected and modified MD calculations for the thermal conductivity of n-dodecane at the temperatures of 500 K and 700 K under different pressures. The pink number indicates AARD value at each operating point between the NIST data and modified MD calculations.

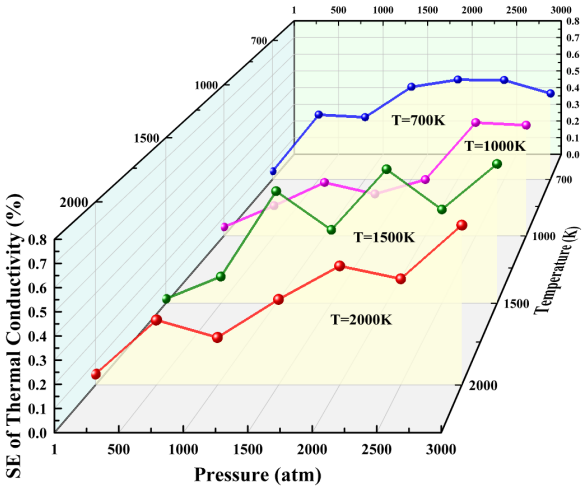

Fig. 19. The SEs of the thermal conductivity calculations for each sampling point of n-dodecane at different pressures and the temperatures ranging from 700 K to 2000 K. Different line colors represent different temperatures, and a series of dots represent the SEs of the modified MD calculated values at all sampling points.

The modified calculations for the viscosity of n-dodecane over a wide temperature and pressure range are provided in Fig. 20. The viscosity is noticeably variable at 298 K and other temperatures, differing at most to two orders of magnitude. At 298 K, the viscosity rises dramatically with increasing pressure. At other temperatures, however, the relationship between the pressure and the viscosity of n-dodecane is much milder, although showing an slight upward trend. Likewise, the viscosity varies widely with temperatures below about 600 K. But in the range above the critical temperature, the magnitude of the change in viscosity with temperatures is significantly diminished. As the temperature rises, the viscosity generally exhibits a declining tendency and drops more slowly.

In the data analysis under the existing working conditions, it is found that the calculation accuracy of n-dodecane viscosity is not as good as that of other thermophysical properties. At a

temperature of 500 K, both the corrected and uncorrected values drastically underestimate the viscosity value, as illustrated in Fig. 21. Despite the fact that the modified results are better than the uncorrected, their AARDs are still significant, at roughly 22 %. Similar to the thermal conductivity, NIST database does not provide the viscosity of n-dodecane at 2500 atm and 3000 atm at 500 K. As a result, SEs are employed in the error analysis under the two working conditions, with a value of 0.002 % at 2500 atm and 0.003 % at 3000 atm. At the temperature of 700 K, the errors of the viscosity are much smaller compared with those at 500 K. The modified results are in better agreement with experimental values than the uncorrected, and the AARD of the corrected viscosity is a maximum of -13.98 % at a pressure of 1500 atm and a minimum of +1.02 % at 2500 atm.

The SEs of the viscosity prediction data are shown in Fig. 22. The SE of viscosity is the smallest of all mentioned thermophysical properties, with a maximum value of only 0.002 %. As can be observed in the graph, the SE of viscosity reduces as the temperature rises, while at the same temperature, the SE shows a growing trend with the increase of the pressure. Therefore, the SE maximum of viscosity occurs in the high pressure and low temperature zone, where the operating point is at a temperature of 700 K and a pressure of 3000 atm.

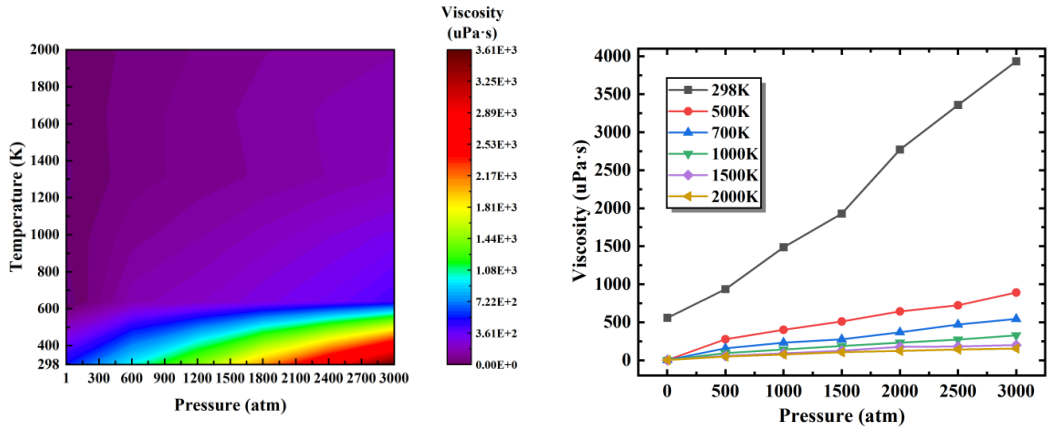

(a) (b)

Fig. 20. The modified results of the viscosity for n-dodecane at the temperatures from 298 K to 2000 K and pressures from 1.2773 atm to 3000 atm using the stability and KDE modifications in the MD simulations.

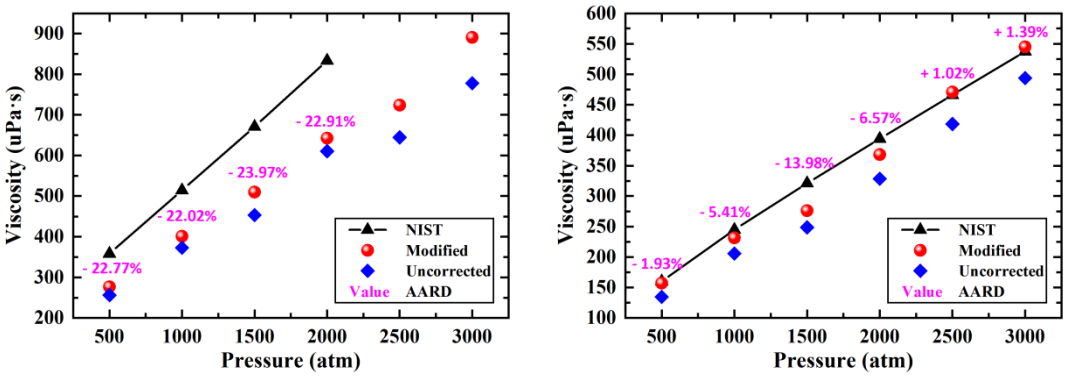

(a) T=500K (b) T=700K

Fig. 21. The comparison of NIST data, uncorrected and modified MD calculations for the viscosity

of n-dodecane at the temperatures of 500 K and 700 K under different pressures. The pink number indicates AARD value at each operating point between the NIST data and modified MD calculations.

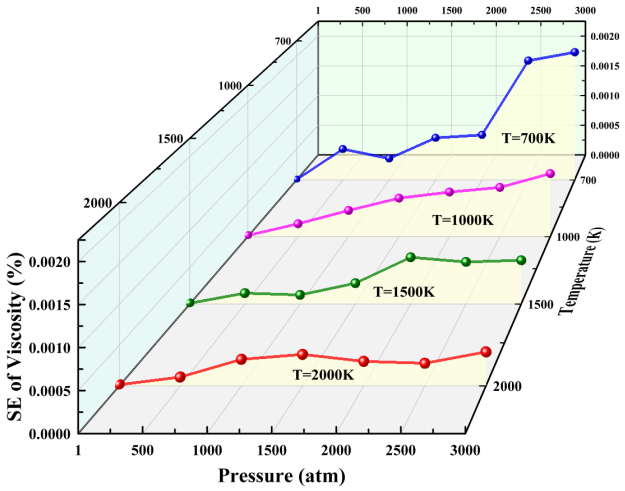

Fig. 22. The SEs of the viscosity calculations for each sampling point of n-dodecane at different pressures and the temperatures ranging from 700 K to 2000 K. Different line colors represent different temperatures, and a series of dots represent the SEs of the modified MD calculated values at all sampling points.

4. Conclusions

In this study, the NPT ensemble and the SKS-UA force field were used to derive the thermophysical parameters of n-dodecane in the temperature range from 298 K to 2000 K and pressure from 1.2773 atm to 3000atm via MD simulation. After integrating the three correction methods in terms of stability correction, KDE correction and zero potential energy surface correction, the initial thermophysical properties results in the aspects of density, internal energy, enthalpy, entropy, thermal conductivity and viscosity were amended. To verify the accuracy of results, AARD was employed for error analysis, while SE analysis was utilized for data under projected conditions. The following are some of the inferences that can be drawn:

(1) For any thermophysical properties of n-dodecane investigated, the results produced by the correction method utilized in this study are closer to the given experimental values than those obtained by conventional MD numerical approach.

(2) The n-dodecane undergoes a supercritical transformation above the critical point, causing its six thermophysical properties to radically change. Density and thermal conductivity are more impacted by pressure, while energy properties in the aspect of internal energy, enthalpy, and entropy are more sensitive to temperature. The viscosity is greatly affected by temperature and pressure below the critical temperature, while almost unaffected above the critical temperature.

(3) In terms of AARD error analysis, the density is in good agreement with the experimental value at given conditions. Regarding energy properties, AARD at low temperature is always larger than that at high temperature and the AARD of entropy is the largest, which could be attributed to the cumulative effect of calculation formula errors and the neglection of Helmholtz free energy. Regarding transport properties, the thermal conductivity matches the experimental value while the viscosity is far underestimated at low temperature.

(4) In the uncertainly analysis of predicted data, the SEs of density and viscosity are minimal and the SE of enthalpy in all thermophysical properties is the highest, but not more than 10 %.

Overall, this research method can be used to predict the six thermophysical properties of n-dodecane in the supercritical state and provides a guiding role in the calculation of thermophysical properties over a wide temperature and pressure range, yielding high-precision thermophysical property calculation results. In addition, the approach developed in this work can be applied to calculate the thermophysical properties of the mono-component to multi-component hydrocarbon fuel in order to achieve thermal properties similar to real fuel.

CRediT authorship contribution statement

Yuanyuan Shen: Methodology, Software, Investigation, Validation, Formal analysis, Writing – original draft. **Chuqiao Wang**: Conceptualization, Supervision, Funding acquisition, Writing – review & editing. **Zhixia He**: Supervision, Funding acquisition, Resources, Writing – review & editing. **Yanzhi Zhang**: Funding acquisition. **Manolis Gavaises**: Conceptualization, Writing – review & editing.

Declaration of Competing Interest

The authors declare that they have no known competing financial interests or personal relationships that could have appeared to influence the work reported in this paper.

Acknowledgments

This work is supported by National Natural Science Foundation of China (Grant No.51776088, No.52106155 and No.52106154).

Appendix A. Supplementary data

Supplementary data to this article can be found online at ..\Supplementary data.docx

References

[1] P. Ni, X. Wang, H. Li, A review on regulations, current status, effects and reduction strategies of emissions for marine diesel engines, Fuel 279 (2020) 118477.
[2] G. Xu, W. Shan, Y. Yu, Y. Shan, X. Wu, Y. Wu, S. Zhang, L. He, S. Shuai, H. Pang, X. Jiang, H. Zhang, L. Guo,S. Wang, F.-S. Xiao, X. Meng, F. Wu, D. Yao, Y. Ding, H. Yin, H. He, Advances in emission control of diesel vehicles in china, Journal of Environmental Sciences (2021).
[3] L. Hao, Z. Zhao, H. Yin, J. Wang, L. Li, W. Lu, Y. Ge, Åke Sjödin, Study of durability of diesel vehicle emissions performance based on real driving emission measurement, Chemosphere 297 (2022) 134171.
[4] M. Wensing, T. Vogel, G. Götz, Transition of diesel spray to a supercritical state under engine conditions,International Journal of Engine Research 17 (2016) 108–119.
[5] S. Xie, Y. Fu, P. Yi, T. Li, R. Chen, Evaluation of trans-critical transition of single- and multi-component sprays under diesel engine-like conditions, Applied Thermal Engineering 202 (2022) 117830.
[6] J. Bellan, Supercritical (and subcritical) fluid behavior and modeling: drops, streams, shear and mixing layers, jets and sprays, Progress in Energy and Combustion Science 26 (2000) 329–366.
[7] J. Safarov, U. Ashurova, B. Ahmadov, E. Abdullayev, A. Shahverdiyev, E. Hassel, Thermophysical properties of diesel fuel over a wide range of temperatures and pressures, Fuel 216 (2018) 870–889.

[8] A. Marmur, Equations of state: Demonstration of a mathematical development methodology, Chemical Engineering Research and Design 178 (2022) 164 – 167.
[9] L. Zheng, A. A. Alhossary, C.-K. Kwoh, Y. Mu, Molecular dynamics and simulation, in: S. Ranganathan, M. Gribskov, K. Nakai, C. Schönbach (Eds.), Encyclopedia of Bioinformatics and Computational Biology, Academic Press, Oxford, 2019, pp. 550 – 566.
[10] I. Koljanin, M. Požar, B. Lovrin ˇ cevi´ c, Structure and dynamics of liquid linear and cyclic alkanes: A molecular dynamics study, Fluid Phase Equilibria 550 (2021) 113237.
[11] K. D. Papavasileiou, L. D. Peristeras, A. Bick, I. G. Economou, Molecular dynamics simulation of pure nalkanes and their mixtures at elevated temperatures using atomistic and coarse-grained force fields, The journal of physical chemistry. B 123 (2019) 6229—6243.
[12] J. P. Ewen, C. Gattinoni, F. M. Thakkar, N. Morgan, H. A. Spikes, D. Dini, A comparison of classical forcefields for molecular dynamics simulations of lubricants, Materials (Basel, Switzerland) 9 (2016).
[13] N. D. Kondratyuk, V. V. Pisarev, Calculation of viscosities of branched alkanes from 0.1 to 1000 mpa by molecular dynamics methods using compass force field, Fluid Phase Equilibria 498 (2019) 151 – 159.
[14] R. Shanthini, Thermodynamics for Beginners - Chapter 4 INTERNAL ENERGY ENTHALPY, 2006, pp. 29 – 34.
[15] T. Zahariev, R. Slavchov, A. Tadjer, A. Ivanova, Fully atomistic molecular-mechanical model of liquid alkane oils: Computational validation, Journal of computational chemistry 35 (2014).
[16] T. Rego, G. M. Silva, M. Goldmann, E. J. Filipe, P. Morgado, Optimized all-atom force field for alkynes within the opls-aa framework, Fluid Phase Equilibria 554 (2022) 113314.
[17] D. N. Bolmatenkov, M. I. Yagofarov, A. A. Notfullin, B. N. Solomonov, Calculation of the vaporization enthalpies of alkylaromatic hydrocarbons as a function of temperature from their molecular structure, Fluid Phase Equilibria 554 (2022) 113303.
[18] K. Sharp, Calculation of molecular entropies using temperature integration, Journal of Chemical Theory and Computation 9 (2013) 1164.
[19] D. Suárez, N. Diaz, Direct methods for computing single-molecule entropies from molecular simulations, Wiley Interdisciplinary Reviews: Computational Molecular Science 5 (2015).
[20] M. Mondello, G. S. Grest, Viscosity calculations of n-alkanes by equilibrium molecular dynamics, The Journal of Chemical Physics 106 (1997) 9327 – 9336.
[21] G. C. da Silva, G. M. Silva, F. W. Tavares, F. P. Fleming, B. A. Horta, Are all-atom any better than united-atom force fields for the description of liquid properties of alkanes? 2. a systematic study considering different chain lengths, Journal of Molecular Liquids 354 (2022) 118829.
[22] X. Yang, M. Zhang, Y. Gao, J. Cui, B. Cao, Molecular dynamics study on viscosities of sub/supercritical ndecane, n-undecane and n-dodecane, Journal of Molecular Liquids 335 (2021) 116180.
[23] G. Galliero, Equilibrium, interfacial and transport properties of n-alkanes: Towards the simplest coarse grained molecular model, Chemical Engineering Research and Design 92 (2014) 3031 – 3037.
[24] C. Chen, X. Jiang, Transport property prediction and inhomogeneity analysis of supercritical n-dodecane by molecular dynamics simulation, Fuel 244 (2019) 48 – 60.
[25] P. Linstrom, E. W.G. Mallard, Nist chemistry webbook, nist standard reference database number 69, national institute of standards and technology, Gaithersburg MD, 20899, Accessed May 11, 2022.

[26] S. A. Mirmohammadi, L. Shen, Y. Gan, A reliable approach for calculating thermophysical properties of liquid using molecular dynamics simulations, Chemical Physics Letters 712 (2018) 44 – 53.
[27] N. Langrené, X. Warin, Fast multivariate empirical cumulative distribution function with connection to kernel density estimation, Computational Statistics Data Analysis 162 (2021) 107267.
[28] F. Kamalov, Kernel density estimation based sampling for imbalanced class distribution, Information Sciences 512 (2020) 1192 – 1201.
[29] D. G. Truhlar, Potential energy surfaces, in: R. A. Meyers (Ed.), Encyclopedia of Physical Science and Technology (Third Edition), third edition ed., Academic Press, New York, 2003, pp. 9 – 17.
[30] R. S. Payal, S. Balasubramanian, I. Rudra, K. Tandon, I. Mahlke, D. Doyle, R. Cracknell, Shear viscosity of linear alkanes through molecular simulations: quantitative tests for n-decane and n-hexadecane, Molecular Simulation 38 (2012) 1234 – 1241.
[31] W. L. Jorgensen, J. D. Madura, C. J. Swenson, Optimized intermolecular potential functions for liquid hydrocarbons, Journal of the American Chemical Society 106 (1984) 6638 – 6646.
[32] J. Siepmann, S. Karaborni, B. Smit, Simulating the critical behaviour of complex fluids, Nature 365 (1993) 330 – 332.
[33] M. G. Martin, J. I. Siepmann, Transferable potentials for phase equilibria. 1. united-atom description of nalkanes, The Journal of Physical Chemistry B 102 (1998) 2569 – 2577.
[34] S. K. Nath, F. A. Escobedo, J. J. de Pablo, On the simulation of vapor – liquid equilibria for alkanes, The Journal of Chemical Physics 108 (1998) 9905 – 9911.
[35] J. N. Israelachvili, 6 - van der waals forces, in: J. N. Israelachvili (Ed.), Intermolecular and Surface Forces (Third Edition), third edition ed., Academic Press, San Diego, 2011, pp. 107 – 132.
[36] İsmail Tosun, Chapter 1 - review of the first and second laws of thermodynamics, in: İsmaıl Tosun (Ed.), The Thermodynamics of Phase and Reaction Equilibria (Second Edition), second edition ed., Elsevier, 2021, pp. 1 – 16.
[37] L. I. Kioupis, E. J. Maginn, Pressure – enthalpy driven molecular dynamics for thermodynamic property calculation: I. methodology, Fluid Phase Equilibria 200 (2002) 75 – 92.
[38] R. Kubo, M. Yokota, S. Nakajima, Statistical-mechanical theory of irreversible processes. ii. response to thermal disturbance, Journal of the Physical Society of Japan 12 (1957) 1203 – 1211.
[39] F. Müller-Plathe, A simple nonequilibrium molecular dynamics method for calculating the thermal conductivity, The Journal of Chemical Physics 106 (1997) 6082 – 6085.
[40] Y. Mao, Y. Zhang, Thermal conductivity, shear viscosity and specific heat of rigid water models, Chemical Physics Letters 542 (2012) 37 – 41.
[41] X. Yang, Y. Gao, M. Zhang, W. Jiang, B. Cao, Comparison of atomic simulation methods for computing thermal conductivity of n-decane at sub/supercritical pressure, Journal of Molecular Liquids 342 (2021) 117478.
[42] A. P. Thompson, H. M. Aktulga, R. Berger, D. S. Bolintineanu, W. M. Brown, P. S. Crozier, P. J. in ’t Veld, A. Kohlmeyer, S. G. Moore, T. D. Nguyen, R. Shan, M. J. Stevens, J. Tranchida, C. Trott, S. J. Plimpton, LAMMPS - a flexible simulation tool for particle-based materials modeling at the atomic, meso, and continuum scales, Comp. Phys. Comm. 271 (2022) 108171.
[43] L. Martínez, R. Andrade, E. G. Birgin, J. M. Martínez, Packmol: A package for building initial configurations for molecular dynamics simulations, Journal of Computational Chemistry 30 2157 – 2164.
[44] C. Chen, X. Jiang, Y. Sui, Prediction of transport properties of fuels in supercritical conditions

by molecular dynamics simulation, Energy Procedia 158 (2019) 1700 – 1705.
[45] Y. Wang, S. Gong, L. Li, G. Liu, Sub-to-supercritical properties and inhomogeneity of jp-10 using molecular dynamics simulation, Fuel 288 (2021) 119696.
[46] J. Fan, S. Liu, C. Gao, F. Song, Molecular dynamic simulation on the transport properties of alcohols, Case Studies in Thermal Engineering 32 (2022) 101888.
[47] Q. Lan, L. Fan, L. Wen, Y. Gu, Y. Wu, J. Li, Multi-factors of fuel injection pressure peak of the pressure amplification common rail fuel system for two-stroke diesel engines, Fuel 321 (2022) 124046.
[48] R. A. Bartolomeu, L. F. Franco, Thermophysical properties of supercritical h2 from molecular dynamics simulations, International Journal of Hydrogen Energy 45 (2020) 16372 – 16380.
[49] F. Cailliez, P. Pernot, Statistical approaches to forcefield calibration and prediction uncertainty in molecular simulation, The Journal of Chemical Physics 134 (2011) 054124.
[50] X. Li, T. Zhan, Y. Zhang, Y. Su, M. He, Y. Zhang, Measurement of the speed of sound in near-critical n-dodecane at temperatures from (433 to 679) k and pressures up to 10.0 mpa, The Journal of Chemical Thermodynamics 170 (2022) 106768.
[51] S. Pronk, S. Páll, R. Schulz, P. Larsson, P. Bjelkmar, R. Apostolov, M. Shirts, J. Smith, P. Kasson, D. van der Spoel, B. Hess, E. Lindahl, Gromacs 4.5: A high-throughput and highly parallel open source molecular simulation toolkit, Bioinformatics (Oxford, England) 29 (2013).
[52] S. Dasari, B. S. Mallik, Conformational dynamics of polymers in ethylammonium nitrate from advanced sampling methods, Computational Materials Science 203 (2022) 111072.
[53] M. Sega, G. Horvai, P. Jedlovszky, On the calculation of the surface entropy in computer simulation, Journal of Molecular Liquids 262 (2018) 58 – 62.
[54] J. Xia, Z. Huang, L. Xu, D. Ju, X. Lu, Experimental study on spray and atomization characteristics under subcritical, transcritical and supercritical conditions of marine diesel engine, Energy Conversion and Management 195 (2019) 958 – 971.